Polyamine−Polycarboxylate Metal Complexes with Different Biological Effectiveness as Nitric Oxide Scavengers. Clues for Drug Design[⊥]

Valentina Bambagioni,[‡] Daniele Bani,*[,†] Andrea Bencini,*[,‡] Tarita Biver,[#] Miriam Cantore,[§] Riccardo Chelli,[‡] Lorenzo Cinci,[†] Paola Failli,*[,§] Lisa Ghezzi,[#] Claudia Giorgi,[‡] Silvia Nappini,[‡] Fernando Secco,[#] Maria Rosaria Tinè,*[,#] Barbara Valtancoli,*[,‡] and Marcella Venturini[#]

Department of Chemistry, University of Florence, Via della Lastruccia 3, Sesto Fiorentino, Florence, Italy, Department of Anatomy, Histology and Forensic Medicine, Section of Histology, University of Florence, V. le G. Pieraccini, 6, Florence, Italy, Department of Chemistry and Industrial Chemistry, University of Pisa, Via Risorgimento 35, Pisa, Italy, and Department of Preclinical and Clinical Pharmacology, University of Florence, V. le G. Pieraccini, 6, Florence, Italy

Received December 12, 2007

The synthesis of the Fe(III), Co(II), Mn(II), and Ru(III) complexes with two polyamine−polycarboxylate ligands, *N*-(2-hydroxyethyl)ethylenediamine-*N*,*N*′,*N*′-triacetic acid (H_3L1) and ethylene bisglycol tetraacetic acid (H_4L2) is reported. Potentiometric studies showed that these ligands form stable complexes in aqueous solution and no metal release occurs, thus accounting for their low toxicity in cultured RAW 264.7 macrophages. X-ray characterization of the $[Co(L1)]^-$ complex showed that binding sites are available at the metal for NO binding. Efficiency of these compounds to bind NO was studied by UV−vis spectrophotometry. Then their NO-scavenging properties were assayed in a cell-free system under physiological conditions, using *S*-nitroso-*N*-acetyl-D,L-penicillamine (SNAP) as NO source. The L1 complexes caused the most effective reduction of free NO, $[Mn(L1)]^-$ being the most efficient. Conversely, in NOS II induced RAW 264.7 macrophages, the Ru(III) and Co(II) complexes with L2 were the most effective compounds. $[Ru(L2)]^-$ also afforded significant protection against lipopolysaccharide-induced endotoxic shock in the mouse in vivo.

Introduction

Nitric oxide (NO[a]) is a gaseous radical well-known to chemists for its high reactivity with both organic and inorganic compounds. In particular, NO can efficiently react with molecules forming complexes with metal ions, such as Fe(II), Co(II), Ru(III), Cu(II), and Mn(II), thus giving rise to stable NO metal nitrosilic adducts.[1] From early 1980s onward, NO has raised an ever-increasing interest in biology and biomedicine after it has been recognized as a novel molecule endogenously synthesized by living organisms with crucial regulatory properties in physiological and pathophysiological conditions.[2] In biological systems, NO is produced by a family of three enzymes, the NO synthases (NOS). Of these, the NOS I and NOS III isoforms are constitutively expressed by a number of cell types (including endothelial cells, neurons, muscle cells, etc.), are susceptible to functional modulation, and generate physiological, nanomolar NO amounts. The third isoform, NOS II, can be genetically induced in many cells (e.g., macrophages and other leukocytes, glial cells, and vascular endothelial and smooth muscle cells) by different stimuli, mainly proinflammatory mediators, and it cannot be functionally modulated and usually generates high micromolar NO amounts.[2,3] In the cell, NO targets chiefly Fe(II) heme containing enzymes, such as guanylyl cyclase and cytochromes, whose activity is thereby modulated, as well as molecular oxygen and reactive oxygen species (ROS).[4] In particular, the reaction of NO with superoxide anion produced at high levels during oxidative stress gives rise to peroxynitrite, a harmful, cytotoxic compound. In fact, NO has been properly defined as a double-edged sword: depending on its concentration and the copresence of NO-reactive substances, it may have beneficial or adverse effects. At low nanomolar levels, NO is a pivotal regulator of vascular tone and organ blood perfusion and acts as a neurotransmitter in the central and peripheral nervous systems.[2,5,6] Conversely, at high micromolar concentrations, NO is deeply involved in inflammatory tissue injury and vascular deregulation, as occurs in chronic inflammatory diseases, neurodegenerative disorders, and circulatory shock.[2,7,8]

One approach for the attenuation of NO-mediated diseases is via NOS inhibition. In this case, the inhibitor shall be selective for NOS II to prevent any deleterious side effect of inhibiting the essential constitutive NOS isoforms. At present, however, no specific NOS II inhibitors are available for clinical use. Some compounds, such as *N*-(3-(aminomethyl)benzyl)acetamidine (1400W), *S*-methyllisothiourea, aminoguanidine, and L-N6-(1-iminoethyl)lysine (L-NIL), show a good NOS II selectivity and currently represent valuable laboratory tools for NO research,[9]

[⊥] The crystallographic data of the structures have been deposited in the Cambridge Crystallographic Data Centre (www.ccdc.cam.ac.uk) and allocated the deposition number CCDC-670134.

* To whom correspondence should be addressed. For D.B.: phone, +390554271390; fax, +390554271385; e-mail, daniele.bani@unifi.it. For A.B.: phone, +390554573371; fax, +390554573365; e-mail, andrea.bencini@unifi.it. For P.F.: phone, +390554271241; fax, +390554271280; e-mail, paola.failli@unifi.it. For M.R.T.: phone, +390502219311; fax, +390502219260; e-mail, mrt@dcci.unipi.it. For B.V.: phone, +390554573274; fax, +390554573365; e-mail, barbara.valtancoli@unifi.it.

[‡] Department of Chemistry, University of Florence.

[†] Section of Histology, University of Florence.

[#] University of Pisa.

[§] Department of Preclinical and Clinical Pharmacology, University of Florence.

[a] Abbrevations: NO, nitric oxide; NOS, NO synthases; ROS, reactive oxygen species; 1400W, *N*-(3-(aminomethyl)benzyl)acetamidine; L-NIL, L-*N*6-(1-iminoethyl)lysine; NaCac, sodium cacodylate $(CH_3)_2AsO_2Na$; SNAP, *s*-nitrosoacetylpenicillamine; PBS, phosphate buffered saline; ATCC, American Type Culture Collection; DMEM, Dulbecco's modified Eagle's medium; TNFα, human recombinant tumor necrosis factor α; INFγ, interferon γ; SEM, standard error of the mean; LPS, lipopolysaccharide.; H_4EDTA, ethylenedinitrilotetraacetic acid; ANOVA, analysis of variance; ip, intraperitoneal; *I*, ionic strength; SCF, self-consistent field; SNAP, *s*-nitroso-*N*-acetyl-D,L-penicillamine; H_5DTPA, diethylentriaminepentaacetic acid; S.S., sickness score.

10.1021/jm701553u CCC: $40.75
Published on Web 05/17/2008

Chart 1. Ligand Drawings

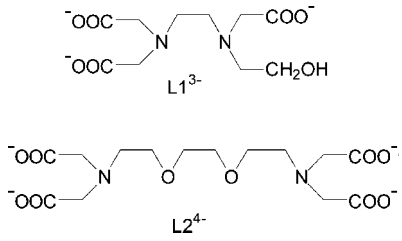

but their actual therapeutic use in humans is limited because most of them can also cause undesired constitutive NOS blockade and hypertension.[10–12]

An alternative therapeutic strategy relies on NO scavengers, low molecular weight compounds potentially capable to remove excess pathogenic NO while leaving enough physiological NO to maintain vascular function. In fact, complexes of Fe(II), Co(II), and Ru(III) with anionic "scaffold" ligands, such as polyamine−polycarboxylates, are currently viewed as effective pharmacological tools to down-regulate endogenously generated NO and promising new drugs for diseases due to NO overproduction.[13,14] An effective NO scavenger should offer substantial advantages over a NOS inhibitor because it does not require enzyme specificity, but it also should meet some major criteria: (i) fast NO reaction kinetics, (ii) activity and stability in biological systems, (iii) lack of toxicity.[15] Moreover, accurate choice and design of the organic scaffold forming complex with the NO-binding metal ions should allow optimization of the pharmacokinetic profile of the whole molecule, adjusting lipophilia and charge accordingly, as well as to increase the reactivity of the metal ion to NO by reducing its charge.

The present study reports on the chemical synthesis and comparative NO-scavenging properties of eight different metal complexes with polyamine−polycarboxylate ligands. Complexes with the selected four metal ions, i.e., Fe(III),[16–20] Co(II),[16,21–24] Mn(II),[16] and Ru(III),[16,25,26] are among the most promising sequestrating agents for NO, both in vitro and in vivo. Although it is known that Fe(III) compounds display a weak tendency to bind NO, it has been reported that Fe(III) complexes can scavenge NO upon reduction to Fe(II) in the intracellular reducing environment, giving rise to effective NO traps in tissues.[17–20] Polyamine−polycarboxylate compounds are generally able to form stable, highly soluble, and low toxic metal complexes. Among these, the two ligands *N*-(2-hydroxyethyl) ethylenediamine-*N*,*N*′,*N*′-triacetic acid (H_3L1) and ethylene bisglycol tetraacetic acid (H_4L2) (Chart 1) would give complexes different coordination geometry, charge, and hydrophobic characteristics. Comparison of the chemical and biological findings obtained with the different compounds allowed us to identify the most suitable ones for pharmacological purposes, as well as to draw useful indications for drug design.

Experimental Section

Compounds $Na_3L1\cdot H_2O$ and H_4L2 as well as the metal salts used were obtained by Aldrich and used without further purification. The aqueous solutions used in complex synthesis, in potentiometric and calorimetric measurements, and in the study of NO binding were deoxygenated by bubbling N_2 in order to avoid possible oxidation of the metals and/or NO.

Synthesis of the Complexes. Na[Co(L1)]·3H$_2$O. A deoxygenated aqueous solution (10 mL) of $CoCl_2\cdot 6H_2O$ (0.24 g, 1 mmol) was slowly added, under stirring, to a boiling solution of $Na_3L1\cdot H_2O$ (0.36 g, 1 mmol) in 20 mL of water under inert atmosphere. The pH was then adjusted at 7 with 0.1 M NaOH. The resulting solution was refluxed for 3 h. The complex was then precipitated by addition of ethanol (30 mL) and recrystallized from a 1:1 H_2O/ethanol mixture. Yield 0.36 g (87.80%). Anal. ($C_{10}H_{21}N_2O_{10}CoNa$) C, H, N.

Crystals of $Na_2[Co(L1)(NCS)]$ were obtained by slow evaporation of an aqueous solution containing $Na[Co(L1)]\cdot 3H_2O$ and NaSCN in equimolecular amounts.

[Co(L1)]·H$_2$O. H_2O_2 (10%, 5 mL) was added to a solution of $Na[Co(L1)]\cdot 3H_2O$ (0.1 g, 0.24 mmol) in 20 mL of water at room temperature. The resulting violet solution was stirred for 12 h. The complex was then precipitated by addition of ethanol (20 mL). Yield 0.075 g (88.75%). Anal. ($C_{10}H_{17}N_2O_8Co$) H, N. C: calcd, 34.10; found, 34.72.

Na[Mn(L1)]. This compound was synthesized from $Na_3L1\cdot H_2O$ (0.36 g, 1 mmol) and $MnSO_4\cdot H_2O$ (0.17 g, 1 mmol) by using the procedure reported for $Na[Co(L1)]\cdot 3H_2O$. Yield 0.25 g (71.42%). Anal. ($C_{10}H_{15}N_2O_7MnNa$) C, H, N.

[Fe(L1)]·2H$_2$O. This compound was synthesized from $Na_3L1\cdot H_2O$ (0.36 g, 1 mmol) and $FeCl_3$ (0.16 g, 1 mmol) by using the procedure reported for $Na[Co(L1)]\cdot 3H_2O$, adjusting pH of the solution to 5. Yield 0.28 g (75.67%). Anal. ($C_{10}H_{19}N_2O_9Fe$) C, H, N.

[Ru(L1)]·H$_2$O. This compound was synthesized in aqueous solution at pH 5 from $Na_3L1\cdot H_2O$ (0.36 g, 1 mmol) and $RuCl_3\cdot H_2O$ (0.22 g, 1 mmol) by using the procedure reported for $Na[Co(L1)]\cdot 3H_2O$, refluxing the solution for 20 h. Yield 0.25 g (64.10%). Anal. ($C_{10}H_{17}N_2O_8Ru$) C, H, N.

Na$_2$[Co(L2)]·2H$_2$O. This compound was synthesized from H_4L2 (0.38 g, 1 mmol) and $CoCl_2\cdot 4H_2O$ (0.20 g, 1 mmol) by using the procedure reported for $Na[Co(L1)]\cdot 3H_2O$. Yield 0.40 g (76.92%). Anal. ($C_{14}H_{24}N_2O_{12}CoNa_2$) C, H, N.

Na$_2$[Mn(L2)]·H$_2$O. This compound was synthesized from H_4L2 (0.38 g, 1 mmol) and $MnSO_4\cdot H_2O$ (0.17 g, 1 mmol) following the procedure for $Na[Co(L1)]\cdot 3H_2O$. Yield 0.34 g (69.39%). Anal. ($C_{14}H_{22}N_2O_{11}MnNa_2$) C, H, N.

Na[Fe(L2)]·4H$_2$O. This compound was synthesized in aqueous solution at pH 5 from H_4L2 (0.38 g, 1 mmol) and $FeCl_3$ (0.16 g, 1 mmol) following the procedure for $Na[Co(L1)]\cdot 3H_2O$. Yield 0.44 g (83.02%). Anal. ($C_{14}H_{28}N_2O_{14}FeNa$) C, H, N.

Na[Ru(L2)]·3H$_2$O. This compound was synthesized in aqueous solution at pH 5 from H_4L2 (0.38 g, 1 mmol) and $RuCl_3\cdot H_2O$ (0.21 g, 1 mmol) following the procedure for $Na[Co(L1)]\cdot 3H_2O$, refluxing the solution for 20 h. Yield 0.39 g (70.91%). Anal. ($C_{14}H_{26}N_2O_{13}RuNa$) C, H, N.

Potentiometric Measurements. All potentiometric measurements ($pH = -\log [H^+]$) were carried out with 0.1 M NMe_4Cl ($pK_w = 13.83$) at 25 ± 0.1 °C by using the previously described equipment and procedure.[27] The computer program HYPERQUAD[28] was used to calculate both protonation and stability constants from emf data.

Microcalorimetric Measurements. The enthalpies of protonation and metal complexation with L1 and L2 were determined in 0.1 M NMe_4Cl aqueous solution by the previously described equipment and procedure.[29] In the protonation and complexation studies 1×10^{-3} M ligand and metal ions concentrations were employed, performing at least three titration experiments. The corresponding enthalpies of reaction were determined from calorimetric data by the AAAL program.[30]

Single Crystal X-Ray Diffraction Analysis. Single-crystal data collection for $Na_2[Co(L1)(NCS)]$ were performed on Xcalibur-Oxford diffractometer using ω scans. The integrated intensities were corrected for Lorentz and polarization effects, and empirical absorption correction was applied by SADABS program. The structure was solved by direct methods (SIR97).[31] Refinement was performed by full-matrix least squares using SHELX-97.[32] All the non-hydrogen atoms were anisotropically refined while the hydrogen atoms were introduced in calculated positions and their coordinates were refined according to the linked atoms. A summary of the crystal data and refinement parameters is given in the Supporting Information (Table S2). The crystallographic data of the structures have been deposited in the Cambridge Crystal-

lographic Data Centre (www.ccdc.cam.ac.uk) and allocated the deposition number CCDC-670134.

Binding of NO. All measurements on the metal complexes interaction with NO were performed at pH 7 and ionic strength $I = 0.11$ M (0.1 M NaCl and 0.01 M NaCac buffer, where NaCac = sodium cacodylate = $(CH_3)_2AsO_2Na$). All solutions were accurately deoxygenated by a nitrogen flow in order to achieve O_2 removal and avoid NO oxidation. Stock solutions of the metal complexes were prepared by dissolving weighed amounts of the solid in the buffer. Working solutions of the appropriate complex concentration were prepared by dilution of the stock solutions with buffer and degassed prior to use. NO aqueous solutions were prepared as reported in ref 33. NO solutions at the desired concentration were obtained by diluting a saturated NO solution (2×10^{-3} M) with appropriately buffered degassed solutions, and NO concentrations were determined with classical methods.[34,35] Doubly deionized water was used to prepare the solutions.

A Perkin-Elmer Lambda 35 spectrophotometer was used to record the absorption spectra and the absorbance variations during titrations. Spectrophotometric titrations were performed by adding increasing volumes of Ru(III) complex solution to the NO solution directly in the degassed spectrophotometric cell using a Hamilton syringe connected to a microscrew (Mitutoyo); the reverse procedure was also employed. Experimental data, recorded at fixed wavelengths, were analyzed by means of nonlinear least-squares fitting procedures (Jandel-AISN). The equilibrium constant was obtained by the iterative procedure described by Hynes and Diebler.[36] All measurements were made at 25.0 ± 0.1 °C.

Kinetics Measurements. The time-course evolution of the $[Co(L1)(NO)]^-$ complex was studied by spectrophotometric measurements on solutions containing the $[Co(L1)]^-$ complex and NO in different molar ratios, monitoring the absorbance at 510 nm. The complex/NO molar ratio was varied from 1:10 to 10:1. The kinetic curves were analyzed by a least-squares procedure. The kinetics of the reaction between the [Ru(L1)] complex and NO were studied using the stopped-flow technique, by monitoring the absorbance changes vs time at $\lambda = 310$ nm and $T = 25.0$ or 4.0 °C after fast mixing of the reactants. The apparatus was equipped with a Biologic SFM-300 mixing unit connected to a spectrophotometric line by optical fibers, as already described.[37] Before each experiment, the mixing unit was degassed using a nitrogen flow. The acquired signal was transferred to a personal computer, and the kinetic curves were analyzed by nonlinear least-squares procedure (Jandel).

Ab Initio Calculations. Ab initio calculations based on the density functional theory have been performed on the $[Co(L1)(NO)]^-$ complex. In particular, we have carried out a structure optimization (via energy minimization) using the B3LYP exchange correlation functional[38,39] and the 6-31G(d,p) basis set. The calculations have been carried out using the Gaussian 03 program.[40] The initial structure for energy minimization was built taking into account the formation of an octahedral cobalt complex with a single NO molecule bound to the metal, as indicated by the solution studies. In this respect we have taken advantage of the structural information available for the $[Co(L1)(NCS)]^-$ complex, simply replacing the Co−NCS moiety with a Co−NO one and fixing the NO oxygen in the original position of NCS carbon atom.

Cell-Free Assay of NO Scavenging by the Metal Ion Compounds. The NO-binding ability of the potential NO-scavenging compounds described above was assayed in a cell-free system. The NO donor *s*-nitrosoacetylpenicillamine (SNAP) (Tocris Cookson, Ellisville, MS), 100 μM, was dissolved in 2 M phosphate buffered saline (PBS), pH 7.4, and incubated for 1 h at 37 °C in the absence or the presence of the Fe(III), Co(II), Mn(II), and Ru(III) complexes with H_4L2 or H_3L1 scaffolds at concentration ranging from 0.1 to 100 μM. The amounts of free NO were evaluated by measuring NO_2^-, the stable oxidation product of NO in aqueous solution, using the Griess reaction. Briefly, 100 μL of reaction mixture was added with 50−100 μL of Griess reagent (1% sulfanilamide and 0.1% *N*-[1-naphthyl]ethylendiamine in 5% phosphoric acid). Incubation was carried out for 30 min in the dark at room temperature. Absorbance was measured at 540 nm wavelength in a Bio-Rad 550 microplate reader. Results are the mean (±standard error of the mean (SEM)) of three independent experiments performed in duplicate and are reported as percent reduction of NO_2^- over the SNAP alone.

In Vitro Culture of RAW 264.7 Macrophages. Murine macrophages RAW 264.7 were obtained from American Type Culture Collection (ATCC, Manassas, VA). Cells were maintained in DMEM (Gibco Invitrogen, CA), supplemented with 10% fetal bovine serum (Gibco), 100 U/mL penicillin−streptomycin, 1% L-glutamine (200 mM), and 4.5 g/L glucose, and grown in 5% CO_2 atmosphere at 37 °C.

Evaluation of NO Produced by Activated RAW 264.7 Macrophages. RAW 264.7 cells were cultured in 24-well plates at 2×10^5 cell/well in 700 μL of Dulbecco's modified Eagle's medium (DMEM) without phenol red and supplemented with 1% fetal bovine serum. The cells were stimulated by 10 μg/ml *E.coli* lipopolysaccharide (LPS) (DIFCO Laboratories, Detroit, MI), 1 ng/mL human recombinant tumor necrosis factor α (TNFα) (Sigma, Milan, Italy), and 100 U/mL human recombinant interferon γ (IFNγ) (Sigma). Eighteen hours after stimulation, NO release in the conditioned medium was evaluated by measuring the accumulation of NO_2^- using the Griess reaction, as described above. The absorbance was measured at 540 nm wavelength in a Bio-Rad 550 microplate reader. To estimate the NO scavenging ability of metal complexes, NO_2^- amounts were measured in RAW 264.7 cells stimulated with the LPS/cytokine cocktail in the absence or the presence of the noted Fe(III), Co(II), Mn(II), and Ru(III) complexes with H_4L2 or H_3L1 scaffolds at concentrations of 50, 100, and 200 μM. For comparison, in parallel experiments, the RAW 264.7 cells were preincubated with 1 μM 1400W (Calbiochem), a highly specific inhibitor of NOS II. Unstimulated RAW 264.7 cells were used to assess basal NO production, which was subtracted from the experimental values. Results are the mean (±SEM) of three independent experiments performed in duplicate and are reported as percent reduction of NO_2^- over the LPS/cytokine-stimulated RAW 264.7 cells not treated with the NO scavengers. Successful NOS II induction by the LPS/cytokine cocktail was assessed by Western blotting in RAW 264.7 cell lysates using a specific anti-NOS II antibody (working dilution, 1:400; Calbiochem, San Diego, CA).

Cytotoxic Assay on RAW 264.7 Cells. RAW 264.7 cells were cultured in 24-well plates (5×10^4 cell/well) in DMEM supplemented with 10% fetal bovine serum as described above. The cells were cultured for up to 96 h in the presence of the noted metal complexes at concentrations ranging from 10 μM to 10 mM.

At 0, 24, 48, 72, and 96 h, the cells were detached using trypsin/EDTA, stained with Trypan blue dye (Biochrom KG, Berlin, Germany), and counted in a Bürker chamber. The percentage of unstained viable cells over the total number of cells was calculated for each experimental set. Results are the mean (±SEM) of triplicate values.

In Vivo NO Scavenging Assay. Male Swiss albino mice (Harlan, Correzzana, Italy) weighing about 30 g were used to assess the efficacy of $Na_2[Co(L2)]\cdot 2H_2O$ and $Na[Ru(L2)]\cdot 3H_2O$ as NO scavengers in an in vivo model of endotoxic shock.[41] They were fed standard laboratory chow and housed under a 12 h light and 12 h dark photoperiod. The experimental protocol complied with the recommendations of the European Economic Community (86/609/CEE) and was approved by the local ethical committee. Briefly, endotoxic shock was induced by intraperitoneal (ip) injection of 24 mg/kg *E. coli* LPS (Difco) in 0.2 mL of PBS. The mice were then divided in 3 groups, 10 animals each. Thirty minutes later, the first group of mice was given an ip injection of 0.2 mL of PBS and used as control. The second group received an ip injection of 50 mg/kg $Na[Ru(L2)]\cdot 3H_2O$ in 0.2 mL of PBS, and the third group received an ip injection of 50 mg/kg $Na_2[Co(L2)]\cdot 2H_2O$ in 0.2 mL of PBS. Injections of PBS or the noted compounds were repeated 24 h later. Concentrations were selected based on preliminary in vivo toxicity experiments with $Na[Ru(L2)]\cdot 3H_2O$ in mice, assessing 60 mg/kg as the higher safe dose (not reported). Mice were scored

Table 1. Thermodynamic Parameters for Co(II), Mn(II), and Fe(III) Complexation with H_3L1 and H_4L2 (I = 0.1 M, 25.0 °C)[a]

reaction	log K	$-\Delta H°$ (kJ mol^{-1})	$T\Delta S°$ (kJ mol^{-1})
$Mn^{2+} + L1^{3-} = [Mn(L1)]^-$	11.56(1)	19.96(7)	45.98(7)
$Co^{2+} + L1^{3-} = [Co(L1)]^-$	14.50(3)	23.0(1)	59.8(1)
$Fe^{3+} + L1^{3-} = [Fe(L1)]$	19.3(1)	38.1(1)	72.0(1)
$Mn^{2+} + L2^{4-} = [Mn(L2)]^{2-}$	12.09(2)	40.6(1)	28.4(1)
$Co^{2+} + L2^{4-} = [Co(L2)]^{2-}$	11.99(4)	13.8(1)	54.4(1)
$[CoL2]^{2-} + H^+ = [Co(HL2)]^-$	4.98(5)	15.9(1)	12.6(1)
$Fe^{3+} + L2^{4-} = [Fe(L2)]^-$	18.42(1)	36.6(1)	68.5(1)

[a] Values in parentheses are standard deviations in the last significant figure.

for sickness severity using the following criteria:[41] score 1 was defined as percolated fur but with no detectable behavior differences compared with control mice; score 2 was defined as percolated fur, huddle reflex, responding to stimuli (such as tap on cage), and just as active during handling as untreated control mice; score 3 was defined as a slower response to tap on cage and passive or docile when handled but still curious when alone in a new setting; score 4 was defined as a lack of curiosity, little or no response to stimuli, and quite immobile; score 5 was defined as labored breathing and unable or slow to self-right after being rolled onto the back (moribund); score 6 was defined as death. Mice were monitored for 74 h. Survival curves and sickness score were calculated for each experimental groups. Significance of differences between the survival curves was evaluated by the χ^2 test.

Statistical Analysis. Results are presented as the mean (±SEM) of biological samples (n).

Unless otherwise stated, differences between the experimental groups were evaluated by two-way analysis of variance ANOVA or one-way ANOVA and Newman−Keuls post-test. Calculations were made with Prism 4 (GraphPad, San Diego, CA) statistical program. A probability value (P) of 0.05 was considered as the lower limit of statistical significant difference.

Results

Synthesis and Characterization of the Complexes. The complexes were prepared by mixing solutions of ligands and metals at neutral pH or, in the case of Ru(III) and Fe(III), at acidic pH values to avoid precipitation of metal hydroxide. The reactions were carried out by using O_2-free solutions to avoid oxidation or O_2 fixation by the Mn(II) and Co(II) complexes. The complexes were characterized by elemental analysis and UV−vis−NIR spectra. Both the Co(II) complexes in aqueous solutions displayed a band in the visible region (λ_{max} = 510 nm, ϵ = 18 cm^{-1} M^{-1} for $[Co(L1)]^-$ and λ_{max} = 520 nm, ϵ = 12 cm^{-1} M^{-1} for $[Co(L2)]^{2-}$) and a broadband in the NIR region at about 1100 nm (ϵ = 5.5 cm^{-1} M^{-1} for $[Co(L1)]^-$ and 4.0 cm^{-1} M^{-1} for $[Co(L2)]^{2-}$), as expected for a high spin Co(II) ion with an octahedral coordination geometry.[42] A charge transfer band was also observed below 250 nm. Instead, as expected for d^5 metal cations, the d−d bands of Mn(II), Fe(III), and Ru(III) were too weak to be monitored in aqueous solution, even at 5 × 10^{-2} M concentrations (the solubility properties of the complexes did not allow us to achieve higher concentrations). The Mn(II) and Fe(III) complexes gave intense and broad charge transfer bands below 250 and 350 nm, respectively. Finally, the [Ru(L1)] complex gave a discrete charge transfer band at 340 nm (ϵ = 1900 cm^{-1} M^{-1}), while $[Ru(L2)]^-$ was characterized by a structured band with two maximum peaks at 304 nm (ϵ = 1381 cm^{-1} M^{-1}) and 360 nm (ϵ = 530 cm^{-1} M^{-1}). The thermodynamic stability of the complexes was studied in aqueous solutions by potentiometric and microcalorimetric titrations in aqueous solutions (0.1 M NMe_4Cl, 25.0 °C), and the results are shown in Table 1. The thermodynamic parameters for ligand protonation reaction are in the range

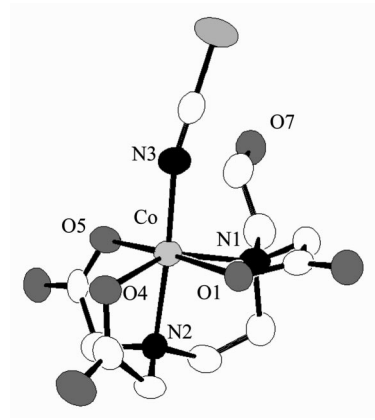

Figure 1. ORTEP drawing of the $[Co(L1)(NCS)]^{2-}$ complex. Bond lengths (Å): Co−N1, 2.184(4); Co−N2, 2.139(4); Co−N3, 2.033(5); Co−O1 2.180(3); Co−O4, 2.083(3); Co−O5, 2.067(4). Bond angles (deg): N3−Co−O5, 97.63(2); N3−Co−O4, 99.24(2); O5−Co−O4, 98.77(1); N3−Co−N2, 176.10(2); O5−Co−N2, 79.95(1); O4−Co−N2, 78.20(1); N3−Co−O1, 86.14(1); O5−Co−O1, 176.08(1); O4−Co−O1, 79.49(1); N2−Co−O1, 96.22(1); N3−Co−N1, 99.60(2); O5−Co−N1, 105.04(2); O4−Co−N1, 147.19(1); N2−Co−N1, 84.02(2); O1−Co−N1, 75.27(1).

generally observed for polyaminocarboxylate ligands[43] and are supplied in the Supporting Information (Table S3). Mn(II), Co(II), and Fe(III) form stable 1:1 complexes with L1 and L2, respectively. Analysis of the species formed in aqueous solution has revealed that Mn(II), Co(II), and Fe(III) only formed complexes with the fully deprotonated forms of ligands complexes, with the exception of the Co(II) complex with L2. In this case, formation of a protonated complex of stoichiometry $[Co(HL2)]^-$ was also observed at acidic pH values. Generally, the metal complexes with both ligands were completely formed in aqueous solutions above pH 4−5 and no free metal was present in solution at neutral pH (see Figures S1 and S2, Supporting Information). In the case of Ru(III), the complexes were completely formed in the pH range (2−11) of our measurements; however, the stability constants are too high to be measured and could only be estimated as higher than 20 log units.

As can be seen from Table 1, both enthalpy and entropic changes promote the formation of all complexes; however, with the only exception of the $[Mn(L2)]^{2-}$, the entropic terms are largely predominant, as expected considering that entropically driven reactions are typical of complexation processes in which charge neutralization plays a mayor role. Finally, when the stability of the different metal complexes is compared, the Fe(III) and Ru(III) form more stable complexes than Co(II) and Mn(II); in fact, the higher positive charge of these metal ions reinforces the electrostatic interactions with the anionic ligands $L1^{3-}$ and $L2^{4-}$ and leads to a more favorable enthalpic contribution to the process of complex formation.

Description of the Crystal Structure of $Na_2[Co(L1)(NCS)]$. The molecular structure consisted of $[Co(L1)(NCS)]^{2-}$ complex anions and Na^+ cations. An ORTEP[44] drawing of the $[Co(L1)(NCS)]^{2-}$ anion is shown in Figure 1. The metal ion is coordinated to the five donor atoms of the ligand, and the coordination sphere is completed by a thiocyanate ion, resulting in distorted octahedral environment. The equatorial plane is defined by the N1, O1, O4, and O5 donors (maximum deviation from the mean plane of 0.217(4) Å for N1). The Co atom lies 0.2111(7) Å from this plane, while N2 and N3 occupy the apical positions. The oxygen atom O7 of the alcoholic pendant arm is

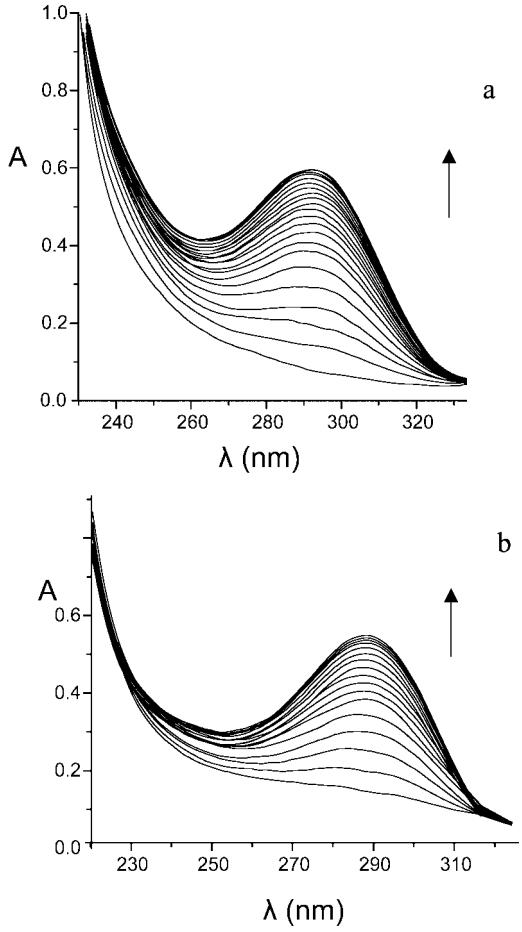

Figure 2. UV spectra recorded on solutions of the $[Co(L1)]^-$ (a) and $[Co(L2)]^{2-}$ (b) (both 5×10^{-3} M) upon successive additions of a NO solution (0.1 equiv each addition) at 25 °C and pH 7.2.

not coordinated to the metal. The Co−N2 and Co−N3 bonds form angles of 5.2(1)° and 8.31(9)°, respectively, with the normal to the basal plane.

Details on the coordination environments of the two Na cations are given within the Supporting Information.

Binding of NO. NO binding to the L1 and L2 metal complexes led to substantial modifications of their UV−vis spectra. In the cases of the Mn(II) and Co(II) complexes, NO binding gave rise to a new intense band at ∼290 nm because of charge transfer processes between the coordinated NO and the metal (see Figure 2 for the Co(II) complexes). Instead, the d−d band in the visible region of the Co(II) complexes only showed minor changes (a slight decrease in molar absorbance and a 3−4 nm blue shift), while the band at 1100 nm remained nearly unchanged. In the case of the Ru(III) complexes, the typical band of the Ru(III) complexes at ∼330 nm tended to disappear upon NO binding, whereas a new band ascribable to [RuL(NO)] complexes (L = L1 or L2) appeared at ∼270 nm (see Figure 3 for the case of the [RuL1(NO)] complex). Similar spectral changes are in accord with those previously reported in the case of the Ru(III) complex with the ethylendiaminetetraacetic acid (H_4EDTA), [Ru(HEDTA)(H_2O)].[15,45] The spectral changes in the UV region can be used to study the NO complex formation equilibria by means of spectrophotometric measurements. In the case of the Fe(III) complexes, no spectral change was observed, even in the presence of a large excess of NO. This suggests that these complexes do not bind or bind very

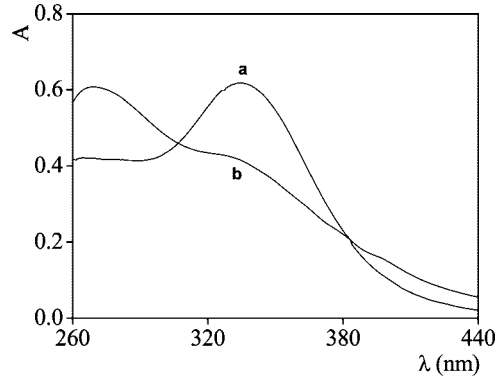

Figure 3. Spectral behavior of the Ru(III)/L1/NO system: pH 7.0, $I = 0.11$ M, $T = 25.0$ °C. (a) UV-vis absorption spectrum of a solution 3.5×10^{-4} M of the [RuL1] complex in the absence of added NO. (b) Absorption spectrum of an equilibrium mixture of [RuL1] (1×10^{-5} M) and [RuL1(NO)] complex (1.9×10^{-4} M).

Table 2. Equilibrium Constants for NO Binding to the Metal Complexes with L1 and L2 ($I = 0.1$ M, 298.1 K)

reaction	K (M^{-1})
$[Mn(L1)]^- + NO = [Mn(L1)(NO)]^-$	$(6.4 \pm 0.3) \times 10^3$
$[Co(L1)]^- + NO = [Co(L1)(NO)]^-$	$(2.4 \pm 0.1) \times 10^4$
$[Ru(L1)] + NO = [Ru(L1)(NO)]$	$(7.2 \pm 0.3) \times 10^4$
$[Mn(L2)]^{2-} + NO = [Mn(L2)(NO)]^{2-}$	$(1.8 \pm 0.1) \times 10^3$
$[Co(L2)]^{2-} + NO = [Co(L2)(NO)]^{2-}$	$(9.2 \pm 0.5) \times 10^3$
$[Ru(L2)]^- + NO = [Ru(L2)(NO)]^-$	$(3.5 \pm 0.4) \times 10^4$

weakly NO, in keeping with the very poor coordination properties of Fe(III) toward this molecule.[1]

In the case of Co(II), Ru(III), and Mn(II), spectrophotometric titrations were carried out at pH 7 either by adding NO solutions to solutions of the complexes or by adding the metal complexes to the NO solutions. The spectrophotometric titrations were treated with the program HYPERQUAD,[28] which allows determination of the stoichiometry of the adducts as well as the addition constants of NO to the metal complexes. As shown in Table 2, all the metal complexes formed stable 1:1 adducts with NO in aqueous solution. The binding ability increased in the order Mn(II) < Co(II) < Ru(III), in keeping with the different reactivity generally described for these metal cations toward small neutral molecules such as NO or CO.[1] At the same time, the L1 complexes displayed a higher affinity for NO than the corresponding L2 ones.

Kinetics Measurements. In the case of the Ru(III) complexes with both ligands and of the Co(II) complex with L1, a slow change of the absorption spectra, in the time range of minutes or hours, is observed after the process of NO binding. For this reason we tried to analyze these systems by means of stopped-flow measurements. In the case of the $[Co(L1)]^-$/NO system, however, the process of NO binding is too fast to be studied by using this technique, even lowering the temperature to 4 °C. The fast binding process is followed by a slow kinetic effect, which is revealed by the spectral evolution shown in Figure 4. A blue shift of the band originally centered at 510 nm, accompanied by a marked absorbance increase, is displayed in the time range of hours. At the same time, the broad band at 1100 nm disappeared. The final spectrum shows an intense single band at 518 nm ($\epsilon = 990$ M^{-1} cm^{-1}). These spectral features resemble in part those of the [Co(III)L1] complex (a single band at 525 nm, $\epsilon = 2190$ M^{-1} cm^{-1}) obtained by direct oxidation of $[Co(II)L1]^-$ with H_2O_2. The time dependence of the spectrum was investigated by recording UV−vis spectra at

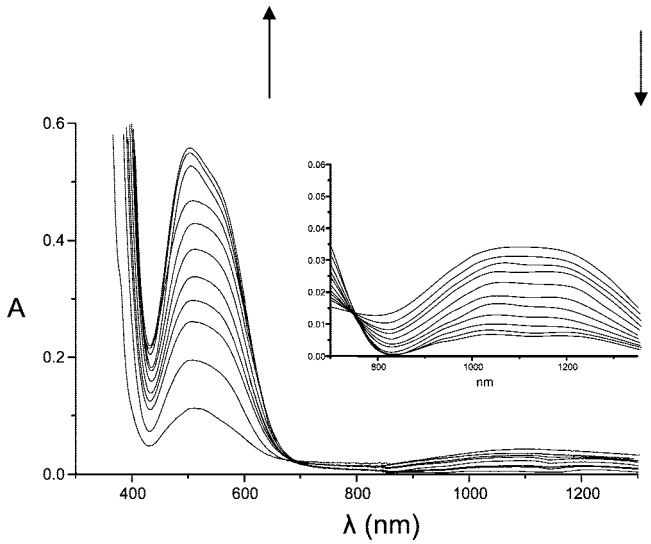

Figure 4. Evolution with time of the absorption spectrum of a solution containing the $[CoL1(NO)]^-$ complex (1×10^{-3} M) (spectra recorded after 1, 2, 2.5, 3.5, 4.5, 6, 7, 9, 12, 16 h). Inset: enlarged view of the NIR region of the absorption spectrum.

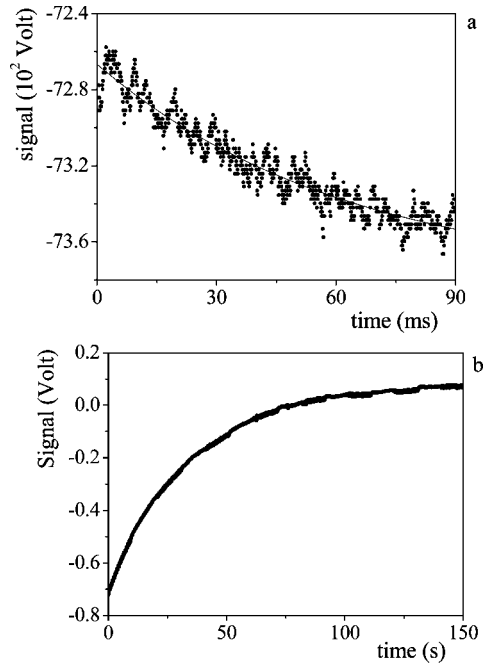

Figure 5. (a) Kinetic curve for the [Ru(L1)]/(NO) system: [Ru(L1)] $= 2.0 \times 10^{-3}$ M, [NO] $= 2.0 \times 10^{-4}$ M, pH 7, $I = 0.11$ M, $T = 4$ °C. The continuous line represents the fit according to monoexponential function. (b) Monoexponential kinetic curve for the [Ru(L1)]/(NO) system: [RuL1] $= 2.0 \times 10^{-3}$ M, [NO] $= 2.0 \times 10^{-4}$ M, pH 7, $I =$ 0.11 M, $T = 25$ °C.

different times on solutions containing NO and the $[Co(L1)]^-$ complex in different molar ratios, i.e., with different concentrations of the $[Co(L1)(NO)]^-$ adduct. Actually, the time constant of the process was found to be independent of the concentration of the $[Co(L1)(NO)]^-$ species, its value being 0.0032 ± 0.0002 min^{-1} at 25 °C.

At 25 °C the process of NO binding to [Ru(L1)] is, once again, too fast to be measured using the stopped-flow method. However, this technique enabled us to measure the rate of formation of the [Ru(L1)(NO)] complex by lowering the temperature to 4 °C. Under pseudo-first-order conditions this reaction is characterized by monoexponential kinetic traces in the time range of hundredths of a second, as that shown in Figure 5a, and their analysis provides an apparent rate constant, k_{obs}, of 16.0 s^{-1} ([Ru(L1)] $= 2.0 \times 10^{-3}$ M, [NO] $= 2.0 \times 10^{-4}$ M, pH 7, ionic strength (I) 0.11 M). Moreover, a monoexponential effect could be observed at 25.0 °C in the time range of minutes, as shown in Figure 5b. The time constant of this effect was found to be independent of the concentration of [Ru(L1)] and equal to 2.9×10^{-2} s^{-1} (pH 7, $I = 0.11$ M). Unfortunately, in the case of the $[Ru(L2)]^-$ complex both the process of NO binding to the complex and its subsequent evolution are too fast to be analyzed even at 4 °C.

Ab Initio Calculations. Two energetic states with different spin multiplicity can be reasonably proposed for Co−NO complexes: a triplet state, formally corresponding to a Co(II)−$NO^{\bullet}$ core, and a singlet state, formally containing a NO^- anion bound to an oxidized Co(III) ion.[16,46] Therefore, calculations of both the singlet-state and the triplet-state optimized geometries of $[Co(L1)(NO)]^-$ have been carried out. Optimization of the singlet state has been accomplished using restricted self-consistent field (SCF) calculations, while for the triplet state both unrestricted and restricted open shell SCF calculations have been attempted. During optimizations of the triplet state, we experienced serious difficulties related to wave function convergence and spin contamination, accounting for an energetic instability of this spin state. Therefore, we are only reporting here the results for the singlet-state geometry, although the existence of a stable triplet state cannot be excluded in principle.

The optimized geometry of $[Co(L1)(NO)]^-$, whose atomic coordinates are available upon request, is shown in Figure 6.

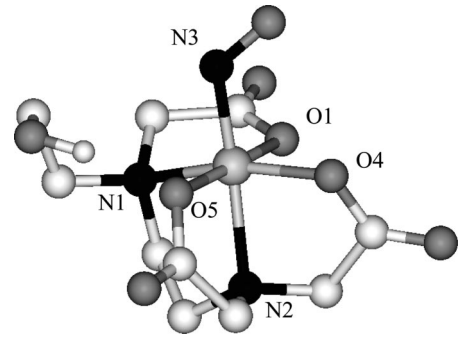

Figure 6. Optimized structure of the $[Co(L1)(NO)]^-$ complex obtained from ab initio calculations. Bond lengths (Å): Co−O1, 1.92; Co−O4, 1.90; Co−O5, 1.94; Co−N1, 2.07; Co−N2, 2.14; Co−N3, 1.80. Bond angles (deg): N1−Co−N2, 86.3; N1−Co−N3, 97.6; N1−Co−O1, 81.0; N1−Co−O5, 95.0; N2−Co−O1, 98.8; N2−Co−O4, 80.5; N2−Co−O5, 80.8; N3−Co−O1, 91.9; N3−Co−O4, 97.7; N3−Co−O5, 88.0; O1−Co−O4, 88.4; O4−Co−O5, 95.5.

Some relevant bonding angles and bond lengths involving Co and the ligand atoms are also reported in the figure. We noticed that ligand atoms form a rather distorted octahedron, in terms of bonding angles. Noteworthy, the Co−N3 bond length was the shortest one (1.8 Å), suggesting the formation of a rather strong interaction between the metal and NO.[1] A further significant feature is that the Co−N−O angle corresponds to a hybrid orbital geometry sp^2, i.e., 119.9°. This structural feature has been already found in other structurally characterized Co−NO cores, such as in nitrosylporphirinato complexes.[46] These results are consistent with an oxidation state of +3 for Co, which implies a partial electron transfer to the NO molecule.[16] In fact, population analysis gave a negative net charge of 0.23 electrons on the NO molecule.

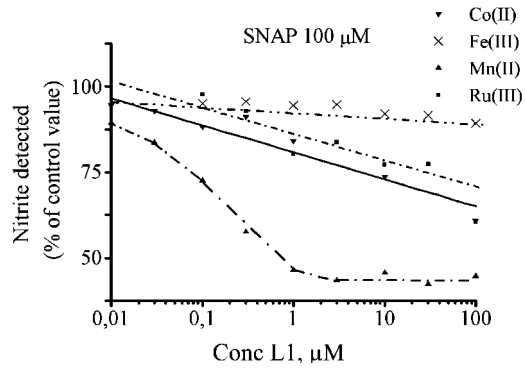

Figure 7. NO-scavenging potency of the studied complexes in the presence of the NO-donor SNAP, evaluated as percent decrease of nitrites, the stable end-products of NO, with respect to the SNAP alone.

NO-Scavenging Properties of the Metal Ion Compounds in Cell-Free System. The compounds under study showed different NO-scavenging potency (Figure 7) when added to a buffer solution at physiological pH, molarity, and temperature and containing a predetermined amount of the NO donor SNAP (100 μM). As shown in Figure 7, within the tested concentration range, all the L1 complexes showed a good dose−effect relationship except for [Fe(L1)], which was virtually devoid of NO-scavenging effects. On the other hand, the spectrophotometric measurements already showed that the Fe(III) complexes do not bind NO. With this notable exception, the compounds with the smaller L1 scaffold appeared to be more potent NO scavengers than their L2-based counterparts. In particular, $[Mn(L1)]^-$ was the most effective compound of the whole experimental set, showing a nearly sigmoidal NO clearance curve with maximal slope being between 0.1 and 1 μM (Figure 7). On the other hand, among the substances with the larger L2 scaffold, $[Ru(L2)]^-$ appeared slightly more potent than $[Mn(L2)]^{2-}$, the percentages of nitrite detected being reduced by 15% and 10%, respectively.

NO-Scavenging Properties of the Metal Ion Compounds on NO Produced by Activated RAW 264.7 Macrophages. Treatment of RAW 264.7 cells with a lipopolysaccharide (LPS)/cytokine cocktail increased the NO_2 production from 1.6 ± 0.4 to 23.7 ± 3.4 nmol/mL ($n = 3$, $P < 0.001$). This increase in NO_2^- production was totally prevented by incubating cells with 1 μM 1400W, suggesting that it was mainly due to NOS II activity. These findings were confirmed by Western blotting, which showed clear-cut NOS II protein induction in the treated RAW 264.7 cells (data not shown). When added to RAW 264.7 cells cultured in vitro upon induction of NOS II by the LPS/cytokine cocktail, the compounds under study showed different NO-scavenging properties. At variance with the findings obtained in the cell-free system, in this cellular model the compounds with the larger L2 scaffold consistently showed a higher NO-scavenging potency than their L1-bearing counterparts (Figure 8). Of note, $[Co(L2)]^{2-}$ and $[Ru(L2)]^-$ showed a fair dose−effect relationship and attained up to 73% and 53% reduction of NO_2^- accumulation, respectively, in the RAW 264.7 cell conditioned medium with the higher concentration (200 μM) compared with the untreated NOS II-induced cells (Figure 8a,b). $[Mn(L2)]^{2-}$ was significantly less potent, whereas $[Fe(L2)]^-$ was nearly ineffective (Figure 8c,d). $[Co(L1)]^-$ and [Ru(L1)] also caused a dose-related reduction of NO_2^- in the medium, but this was never higher than 25% of the values of the untreated NOS II-induced cells, whereas $[Mn(L1)]^-$ and [Fe(L1)] were ineffective (Figure 8).

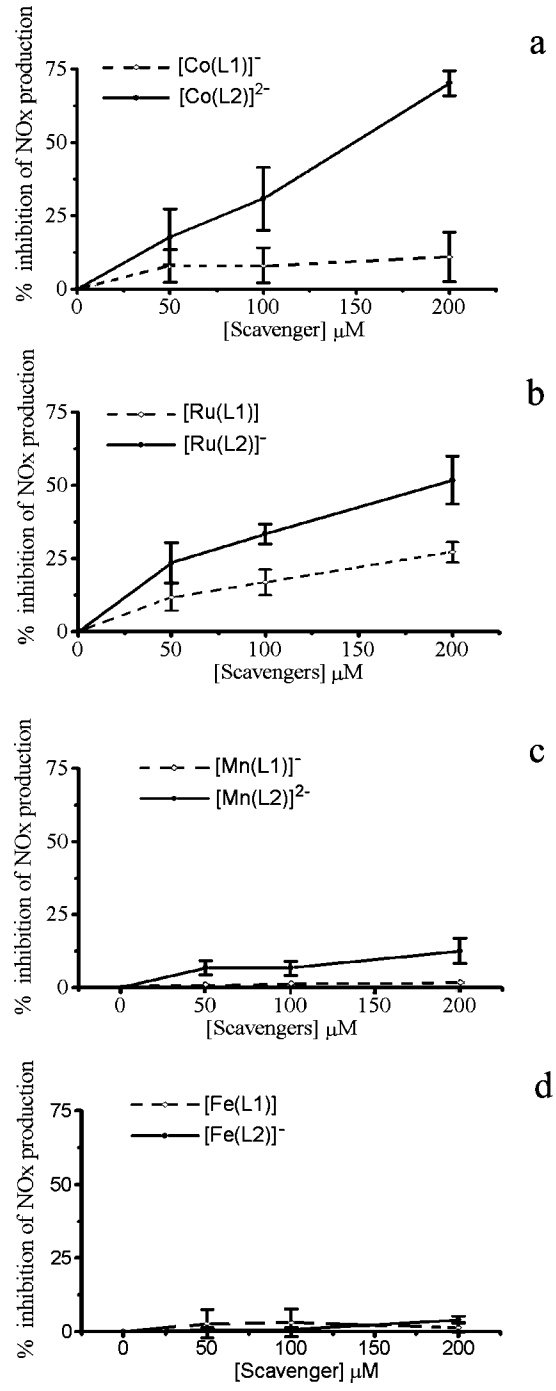

Figure 8. NO-scavenging potency of the Co(II) (a), Ru(III) (b), Mn(II) (c), and Fe(III) (d) complexes added to the culture medium of activated RAW 264.7 macrophages, expressed as percent inhibition of the accumulation of nitrites, the stable end-products of NO.

Cytotoxic Effects of the NO Scavengers on RAW 264.7 Cells. To rule out the possibility that decreased NO in the conditioned medium could be related to toxic effects of the NO scavengers on RAW 264.7 macrophages, we carried out a time-course cytotoxicity test by staining the cells with Trypan blue vital dye, using $[Co(L2)]^{2-}$ and $[Ru(L2)]^-$ as representative molecules. This choice was based on the higher NO scavenging efficiency of these complexes compared with the other tested compounds. Addition of $[Co(L2)]^{2-}$ at concentrations of 10 and 100 μM to the culture medium of RAW 264.7 cells for up to 96 h did not decrease the percentage of viable cells compared with the untreated control cultures. Significant cytotoxic effects

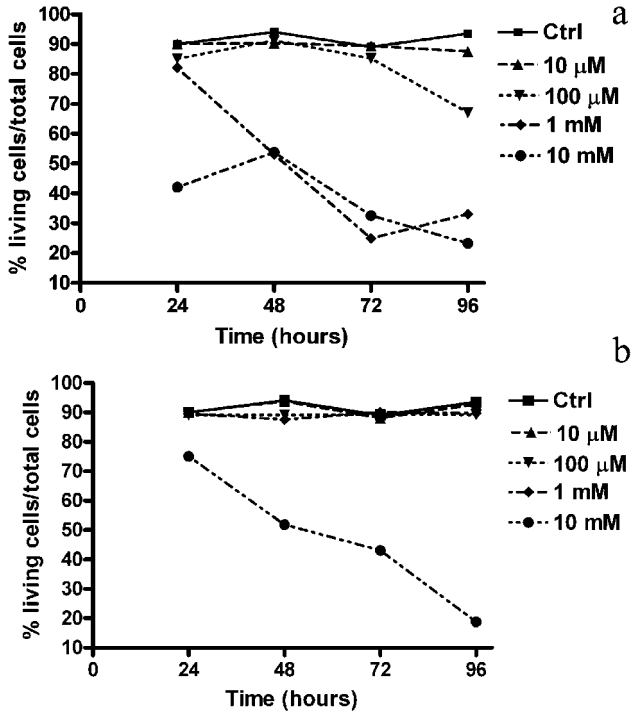

Figure 9. Cytotoxicity of the NO scavengers $[Co(L2)]^{2-}$ (a) and $[Ru(L2)]^{-}$ (b), added at the noted concentrations and incubation times to the culture medium of RAW 264.7 macrophages, expressed as percent viable cells over the total cells.

were only observed at the higher 1 and 10 mM concentrations of this compound (Figure 9a). On the other hand, $[Ru(L2)]^{-}$ had no cytotoxic effects at 10 μM, 100 μM, and 1 mM, only causing a decrease in cell viability at the highest 10 mM concentration (Figure 9b).

Protection Afforded by the Metal Ion Compounds on LPS-Induced Endotoxic Shock in Vivo. We eventually investigated whether $Na_2[Co(L2)]\cdot 2H_2O$ and $Na[Ru(L2)]\cdot 3H_2O$, which had shown the highest NO-scavenging potency in the in vitro test with RAW 264.7 macrophages, could also have therapeutic effects when given systemically to mice undergoing LPS-induced endotoxic shock, a well-known NO-driven disease. For the current experiments, a single dose of 24 mg/kg LPS induced clear-cut signs of sickness in all the mice within 12 h and was lethal for 80% of the vehicle-treated control mice by 74 h. Administration of $Na[Ru(L2)]\cdot 3H_2O$ (50 (mg/kg)/day for 2 days) to mice after induction of the shock syndrome by LPS significantly increased the survival rate to 90% at variance with the 20% of the vehicle-treated controls ($p < 0.01$) and reduced the overall sickness score. On the other hand, $Na_2[Co(L2)]\cdot 2H_2O$ given at the same dose as $Na[Ru(L2)]\cdot 3H_2O$ had far lower effects, being only capable of increasing the survival rate to 40% (Figure 10).

Discussion

The present study offers further evidence for the effectiveness of metal ion complexes with polyamine−polycarboxylate scaffolds as NO scavengers capable of removing excess NO in biological systems. In aqueous solutions at physiological pH, temperature, and molarity, the tested ligands form stable complexes with Fe(III), Co(II), Mn(II), and Ru(III) and do not release detectable metal ion amounts. With the exception of the Fe(III) complexes, all the metal ions under investigation form stable adducts with NO; for both the L1 and L2 complexes, the

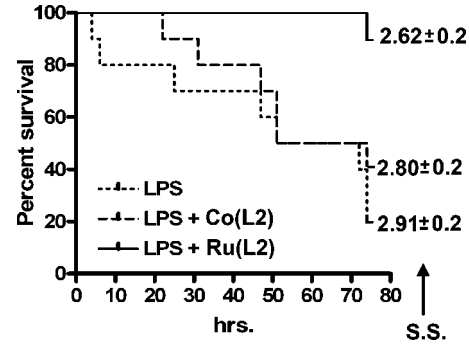

Figure 10. In vivo effects of the NO scavengers $Na_2[Co(L2)]\cdot 2H_2O$ and $Na[Ru(L2)]\cdot 3H_2O$ (indicated as Co(L2) and Ru(L2)) administered therapeutically to mice undergoing LPS-induced endotoxic shock (each group, $n = 10$). Survival curves are expressed as percent of animals that survived at 74 h (S.S., sickness score (mean ± SEM)).

binding affinity increases in the order Mn(II) < Co(II) < Ru(III). The lack of reactivity of Fe(III), as well as the observed increasing binding affinity from Mn(II) to Ru(III), reflects the reactivity toward NO, CO, and other π-acceptor molecules displayed by these metal cations and their complexes.[1] At the same time, for all the metal cations under study, the L1 complexes display a higher affinity for NO than the L2 ones. This behavior can be related to the different structure and number of donor atoms of the two ligands. Actually, ligand L2 is characterized by a larger number of donors and by a more flexible backbone, which would allow "envelopment" of the metal ion. For instance, a previously reported crystal structure of the Mn(II) complex[47] shows that the metal is octacoordinated by the L2 donors and is almost embedded by the ligand. In contrast, L1 possesses only five coordinating groups, i.e., the three carboxylate groups and the two nitrogens, available for metal binding. As shown by the crystal structure of the $[Co(L1)(NCS)]^{2-}$ complex, the ligand donors do not saturate the coordination sphere of the metal and leave a binding site on the metal that can be used for coordination of exogenous species, such as a thiocyanate anion. Most likely, in aqueous solution in the absence of SCN^{-}, this binding zone is occupied by a water molecule, which can be easily replaced by NO. This would explain the higher affinity of the L1 complexes for NO. Interestingly, the binding constants of NO to the [Ru(L1)] and $[Ru(L2)]^{-}$ complexes are remarkably lower than that reported for the Ru(III) complex with EDTA, $[Ru(HEDTA)(H_2O)]$ ($K > 10^8\ M^{-1}$),[15] but only slightly lower than that found for the Ru(III) complex with diethylentriaminepentaacetic acid (H_5DTPA),[15] $[Ru(H_3DTPA)Cl]^{3-}$ ($K = 2 \times 10^{-5}\ M^{-1}$), one of the most efficient NO scavenger in RAW 264.7 macrophage cell line (see below).

Concerning the kinetic aspects of the present study, we have found that NO binding to the $[Co(L1)]^{-}$ complex is too fast to be studied by using the stopped-flow method, even lowering the temperature to 4 °C. On the other hand, binding of NO to give the $[Co(L1)NO]^{-}$ complex is followed by a slow intramolecular process; the temporal evolution of absorption spectra, which takes place in some hours, gives rise to a final spectrum characterized by a single absorption band at 518 nm ($\epsilon = 990\ M^{-1}\ cm^{-1}$). These spectral features are typical of Co(III) complexes. In the case of cobalamines, it has been reported that NO binding is followed by oxidation of Co(II) to Co(III) with the formation of a Co−NO complex formally containing Co(III).[48,49] In our case, however, the absorbance at 518 nm is lower than that measured for the [Co(III)L1] complex ($\epsilon = 2190\ M^{-1}\ cm^{-1}$), obtained by oxidation of $[Co(II)(L1)]^{-}$ with H_2O_2,

suggesting that only a partial charge transfer takes place between the metal center and NO. This fact is confirmed by ab initio calculations that show that only a negative net charge of 0.23 electrons is localized on the NO molecule. The measured first-order rate constant (0.0032 ± 0.0002 min^{-1}) is too low for a simple intramolecular electron transfer process, which is generally characterized by far higher rate constants.[50] Most likely, the electron transfer from the metal to NO is coupled with a simultaneous process of rearrangement of the ligand around the coordination sites of the oxidized metal cation. This rearrangement could imply an intramolecular dissociation−reassociation process of some of the chelating units of L1, which could justify the slowness of the monomolecular step shown in Figure 4. From this point of view, similar ligand rearrangements around cobalt are known and generally involve intramolecular equatorial−equatorial or axial−equatorial interchange of chelating groups.[51] On the basis of these considerations, an intramolecular interchange between two donor atoms, such as an amine nitrogen and a carboxylate oxygen of L1, within the metal coordination environment may be reasonably proposed to explain the observed slow monomolecular process.

It is of interest to note that the NO adduct with the L2 complex does not show any tendency to give metal oxidation probably because of the presence of a hydrophobic polyether chain. It is known, in fact, that the presence of hydrophobic moieties close to metal centers can hinder redox processes. Substitution reaction at the Ru(III) centers is generally a much slower process compared to substitution at Co(II). Actually, the stopped-flow study of the reaction of [Ru(L1)] with NO shows that the process is biphasic. The fast phase corresponds to the substitution by NO of the H_2O molecule coordinated at the metal center. This process appears to be remarkably faster compared to the process of water exchange at the $[Ru(H_2O)_6]^{3+}$ ion ($k_{H2O} = 10^{-6}$ s^{-1}),[52] as expected considering the labilization of the coordination sphere induced in tervalent metal ions by already coordinated ligands.[53] It has been reported that NO binding by Ru(III) complexes with polyamine−polycarboxylate ligands, such as EDTA and DTPA, is accompanied by charge transfer from NO to the Ru(III) center to give a complex in a Ru(II)−NO^+ formal oxidation state.[13,25,26] On the other hand, the second relatively slow phase observed in our case cannot be simply due to an intramolecular charge transfer, since these processes are remarkably faster, even faster than the process of binding to the metal.[50] Therefore, this process can be reasonably ascribed to a conformational change of the [Ru(L1)NO] complex formed in the fast step, similar to that proposed for the corresponding cobalt complex. From this point of view, intramolecular axial−equatorial or equatorial−equatorial ligand interchange is also known in the cases of Ru(III) and Ru(II).[54,55] Owing to the ability of Ru(III) to withdraw electrons from NO, we favor the view that charge transfer and conformation change are strongly coupled, as actually observed in the case of the Co(II) complex. On the basis of the above considerations, the reaction mechanism for the [Ru(L1)]/NO system can be represented by the following:

$$[(H_2O)Ru(L1)] + NO \rightleftharpoons [(NO)Ru(L1)]_a \rightleftharpoons [(NO)Ru(L1)]_b$$

where the ternary complex $[(NO)Ru(L1)]_a$ differs from complex $[(NO)Ru(L1)]_b$ in geometry and charge distribution.

From a biological/pharmacological perspective, the current finding that at physiological pH, temperature, and molarity, the tested Fe(III), Co(II), Mn(II), and Ru(III) complexes are highly stable and do not release detectable metal ion amounts can account for their low cytotoxicity. For instance, [RuL1] only showed significant cytotoxic effects at 10 mM, far above its concentration range as effective NO scavenger. Taken together, the above findings provide support to the concept that such molecules could be the basis for the development of new drugs for causative therapy of diseases related to NO hyperproduction.[2,7,8] This view is further strengthened by the current in vivo findings, which offer preliminary evidence for a therapeutic action of $[Ru(L2)]^-$ and at a lesser extent $[Co(L2)]^{2-}$, taken as representative compounds based on their efficacy as NO scavengers in vitro, on experimentally induced septic shock syndrome in mice. Moreover, our study first shows that NO-scavenging properties can differ depending on the selected metals and scaffolds, as well as on the environmental conditions in which the reaction between the compounds and NO occurs. Actually, in a cell-free system, in which the reaction parameters were set to roughly reproduce the physiological conditions, the $[Mn(L1)]^-$ complex was the most effective NO-scavenging compound and, overall, the L1 scaffold appeared to offer a substantial advantage over L2. Conversely, in NOS II induced RAW 264.7 macrophages $[Co(L2)]^{2-}$ and $[Ru(L2)]^-$ were the most effective compounds and, overall, the L2 scaffold gave better performance than L1. As discussed above, this peculiar behavior is likely related to the different structural characteristics of L1 and L2. In particular, the larger number of donors and the more flexible and hydrophobic backbone of L2 reduce the binding ability of its complexes toward NO and, at the same time, hinder possible processes of oxidation of the metals. Conversely, this apparently negative chemical feature of L2 may paradoxically become favorable in an oxidant environment, as occurs in LPS/cytokine-stimulated RAW 264.7 macrophages. In these cells, besides NOS II, proinflammatory stimuli can induce an oxidative burst, resulting in the formation of large amounts of ROS. In this context, L2 could protect the metal center from oxidation better than could L1, thereby preventing oxidation-induced inactivation of the NO-coordinating properties of the metal. Indirect support of this hypothesis comes from the observation that under any condition tested the Fe(III)-containing compounds are nearly ineffective as NO scavengers; Fe(III) complexes, in fact, were found active as NO scavengers in intracellular reducing environments because of reduction of Fe(III) to Fe(II), which generally displays a high affinity for NO.[17−20] Most likely, in the oxidant environment of our cell cultures, Fe(III) reduction is inhibited, leading to the observed inability in NO trapping of the Fe(III) complexes.

The present findings are consistent with the previously described properties of Ru(III) complexes with other polyamine−polycarboxylate ligands, such as EDTA and DTPA, which have been recently studied as NO scavengers in NOS II induced RAW 264.7 macrophages.[15,56] Of note, the most efficient scavenger is the $[Ru(H_3DTPA)Cl]$ complex, which shows a NO-scavenging potency similar to that of $[Ru(L2)]^-$ and $[Co(L2)]^{2-}$ at a 100 μM concentration but appears less potent than these two complexes at a higher 200 μM concentration (reduction of nitrite accumulation: $[Ru(H_3DTPA)Cl]$, 41%; $[Ru(L2)]^-$, 53%; $[Co(L2)]^{2-}$, 73%).

In conclusion, the present study provides a detailed chemical characterization of Fe(III), Co(II), Mn(II), and Ru(III) metal ion complexes with polyamine−polycarboxylate ligands L1 and L2 and offers evidence for their pharmacological properties as NO scavengers both in vitro on inflammation-activated macrophages and in vivo on mice undergoing LPS-induced septic shock syndrome, thus validating their therapeutic potential. On the basis of the reported data, $[Co(L2)]^{2-}$ and $[Ru(L2)]^-$ appear as the most potent NO scavengers of the tested compounds, but

the latter one emerges as the best candidate as a possible NO-scavenging drug because of its lower cytotoxic profile and higher in vivo efficacy. The current findings provide the necessary background to further studies on animal models of disease by excess endogenous NO generation, which could provide characterization of the in vivo toxicity, pharmacokinetic, and pharmacodynamic profiles of these compounds as well as of the spectrum of their possible therapeutic applications.

Acknowledgment. We thank Prof. Gianni Cardini (Department of Chemistry, University of Florence) for the helpful suggestions on ab initio calculations. R.C.'s work was supported by the European Union (Contract RII3-CT-2003-506350).

Supporting Information Available: Elemental analysis of the complexes, thermodynamic parameters for protonation of L1 and L2, distribution diagrams of the L1 and L2 complexes, summary of crystal data and of refinement parameters, and details of the coordination environments of the sodium cations in the crystal structure of $Na_2[Co(L1)(NCS)]$. This material is available free of charge via the Internet at http://pubs.acs.org.

References

(1) Cotton, F. A.; Wilkinson, G. *Advanced Inorganic Chemistry*; John Wiley & Sons: New York,1988.
(2) Moncada, S.; Palmer, R. M. J.; Higgs, E. A. Nitric oxide physiology, pathophysiology, and pharmacology. *Pharmacol. Rev.* **1991**, *43*, 109–142.
(3) Nathan, C. Nitric oxide as a secretory product of mammalian cells. *FASEB J.* **1992**, *6*, 3051–3064.
(4) Ignarro, L. Signal transduction mechanisms involving nitric oxide. *Biochem. Pharmacol.* **1991**, *41*, 485–490.
(5) Feng, Q.; Hedner, T. Endothelium-derived relaxing factor (EDRF) and nitric oxide (NO). I. Physiology, pharmacology and pathophysiological implications. *Clin. Physiol.* **1990**, *10*, 407–426.
(6) Lowenstein, C. J. Dinerman, J. L., Snyder, S. H. Nitric oxide: a physiologic messenger. *Ann. Intern. Med.* **1994**, *120*, 227–237.
(7) Thiemermann, C. The role of the L-arginine: nitric oxide pathway in circulatory shock. *Adv. Pharmacol.* **1994**, *28*, 45–79.
(8) Moncada, S. Higgs, E. A. Molecular mechanisms and therapeutic strategies related to nitric oxide. *FASEB J.* **1995**, *9*, 1319–1330.
(9) Salerno, L.; Sorrenti, V.; Di Giacomo, C.; Romeo, G.; Siracusa, M. A. Progress in the development of selective nitric oxide synthase (NOS) inhibitors. *Curr. Pharm. Des.* **2002**, *8*, 177–200.
(10) Yates, D. H.; Kharitonov, S. A.; Thomas, P. S.; and Barnes, P. J. Endogenous nitric oxide is decreased in asthmatic patients by an inhibitor of inducible nitric oxide synthase. *Am. J. Respir. Crit. Care Med.* **1996**, *154*, 247–250.
(11) Cobb, J. P. Nitric oxide synthase inhibition as therapy for sepsis: a decade of promise. *Surg. Infect. (Larchmt.)* **2001**, *2*, 93–100.
(12) Hansel, T. T.; Kharitonov, S. A.; Donnelly, L. E.; Erin, E. M.; Currie, M. G.; Moore, W. M.; Manning, P. T.; Recker, D. P.; Barnes, P. J. A selective inhibitor of inducible nitric oxide synthase inhibits exhaled breath nitric oxide in healthy volunteers and asthmatics. *FASEB J.* **2003**, *17*, 1298–1300.
(13) Fricker, S. P. Metal Ions and Their Complexes in Medication. In *Metal Ions in Biological Systems*; Sigel, A., Sigel, H. Eds.; Marcel Dekker: New York, 2004; Vol. 41, pp 421−480.
(14) Fricker, S. P. Nitric oxide scavengers as a therapeutic approach to nitric oxide mediated disease. *Expert Opin. Invest. Drugs* **1999**, *8*, 1209–1222.
(15) Cameron, B. R.; Darkes, M. C.; Yee, H.; Olsen, M.; Fricker, S. P.; Skerlj, R. T.; Bridger, G. J.; Davies, N. A.; Wilson, M. T.; Rose, D. J.; Zubieta, J. Ruthenium(III) polyaminocarboxylate complexes: efficient and effective nitric oxide scavengers. *Inorg. Chem.* **2003**, *42*, 1868–1876.
(16) McCleverty, J. A. Chemistry of nitric oxide relevant to biology. *Chem. Rev.* **2004**, *104*, 403–418.
(17) Kazmeirski, W. M.; Wolberg, G.; Wilson, J. G.; Smith, S. R.; Williams, D. S.; Thorp, H. H.; Molina, L. Iron chelates bind nitric oxide and decrease mortality in an experimental model of septic shock. *Proc. Natl. Acad. Sci. U.S.A.* **1996**, *93*, 9138–9141.
(18) Lai, C. S.; Komarov, A. Detection of nitric oxide spin trapping of nitric oxide produced in vivo in septic-shock mice. *FEBS Lett.* **1994**, *345*, 120–124.
(19) Lai, C. S.; Komarov, A. Production in mice by spin-trapping electron paramagnetic resonance spectroscopy. *Biochim. Biophys. Acta* **1995**, *1272*, 29–36.
(20) Mikoyan, V. D.; Kubrina, L. N.; Serezhenkov, V. A.; Stukan, R. A.; Vannin, A. F. Complexes of Fe^{2+} with diethyldithiocarbamate or *N*-methyl-D-glucamine dithiocarbamate as traps of nitric oxide in animal tissues: comparative investigations. *Biochim. Biophys. Acta* **1997**, *1336*, 225–234.
(21) Rajanayagam, M. A. S.; Li, C. G.; Rand, M. J. Differential effects of hydroxoxobalamin on nitric oxide-mediated relaxations in rat aorta and anococygeus muscle. *Br. J. Pharmacol.* **1993**, *108*, 3–5.
(22) Greenberg, S. S.; Xie, J.; Zatarain, J. M.; Kapusta, D. R.; Miller, M. S. Hydroxocobalamin (vitamin B12a) prevents and reverses endotoxin-induced hypotension and mortality in rodents: role of nitric oxide. *J. Pharmacol. Exp. Ther.* **1995**, *273*, 257–265.
(23) Wolak, M.; Zahl, A.; Schneppensieper, T.; Stochel, G.; van Eldik, R. Kinetics and mechanism of the reversible binding of nitric oxide to reduced cobalamin B12r (CoB(II)alamin). *J. Am. Chem. Soc.* **2001**, *123*, 9780–9791.
(24) Zheng, D.; Yan, L.; Birke, R. L. Electrochemical and spectral studies of the reactions of aquocobalamin with nitric oxide and nitrite ion. *Inorg. Chem.* **2002**, *41*, 2548–2555.
(25) Bottomley, F. Nitrosyl complexes of ruthenium. *Coord. Chem. Rev.* **1978**, *26*, 7–32.
(26) Seddon, E. A.; Seddon, K. R. *The Chemistry of Ruthenium*; Elsevier: Amsterdam, 1984.
(27) Lodeiro, C.; Parola, A. J.; Pina, F.; Bazzicalupi, C.; Bencini, A.; Bianchi, A.; Giorgi, C.; Masotti, A.; Valtancoli, B. Protonation and Zn(II) coordination by dipyridine-containing macrocycles with different molecular architecture. A case of pH-controlled metal jumping outside−inside the macrocyclic cavity. *Inorg. Chem.* **2001**, *40*, 2968–2975.
(28) Gans, P.; Sabatini, A.; Vacca, A. Investigation of equilibria in solution. Determination of equilibrium constants with HYPERQUAD suite of programs. *Talanta* **1996**, *43*, 1739–1753.
(29) Bazzicalupi, C.; Bencini, A.; Fusi, V.; Giorgi, P.; Paoletti, P.; Valtancoli, B. Lead complexation by novel phenanthroline-containing macrocycles. *J. Chem. Soc., Dalton Trans.* **1999**, 393–400.
(30) Vacca, A. *AALL Program*; University of Florence: Florence, Italy, 1997.
(31) Altomare, A.; Burla, M. C.; Cavalli, M.; Cascarano, G. L.; Giacovazzo, C.; Guarlandi, A.; Moliterni, A. G. G.; Polidori, G.; Spagna, R. SIR97: a new tool for crystal structure determination and refinement. *J. Appl. Crystallogr.* **1999**, *32*, 115–119.
(32) Sheldrick, G. M. *SHELXL-97*; University of Göttingen: Göttingen, Germany, 1997.
(33) Fernelius, W. C. Ed. *Nitric Oxide, Inorganic Synthesis*; MacGraw-Hill Book Companies: New York, 1946; Vol. 2, Chapter V, pp 126−142.
(34) Feelisch, M., Stamler, J. Eds. *Methods in Nitric Oxide Research*; John Wiley & Sons Ltd.: West Sussex, U.K., 1996.
(35) Torres, J.; Wilson, M. T. *Methods in Enzymology*; Academic Press: San Diego, CA, 1996; Vol. 269.
(36) Hynes, M. J.; Diebler, H. The binding of Ni^{2+} to adenylyl-3′,5′-adenosine and to polyadenylic acid. *Biophys. Chem.* **1982**, *16*, 79–88.
(37) Garcia, B.; Gonzalez, S.; Hoyuelos, J.; Ibeas, S.; Leal, J. M.; Senent, M. L.; Biver, T.; Secco, F.; Venturini, M. Thermodynamics and kinetics of the nickel(ii)-salicylhydroxamic system. Phenol rotation induced by metal ion binding. *Inorg. Chem.* **2007**, *46*, 3680–3687.
(38) Becke, A. D. Density-fuctional exchange−energy approximation with correct asymptotic behavior. *Phys. Rev. A* **1988**, *33*, 3098–3100.
(39) Lee, C.; Yang, W.; Parr, R. G. Development of the Colle−Salvetti correlation-energy formula into a functional of the electron density. *Phys. Rev. B* **1988**, *37*, 785–789.
(40) Frisch, M. J.; Trucks, G. W.; Schlegel, H. B.; Scuseria, G. E.; Robb, M. A.; Cheeseman, J. R.; Montgomery, J. A., Jr.; Vreven, T.; Kudin, K. N.; Burant, J. C.; Millam, J. M.; Iyengar, S. S.; Tomasi, J.; Barone, V.; Mennucci, B.; Cossi, M.; Scalmani, G.; Rega, N.; Petersson, G. A.; Nakatsuji, H.; Hada, M.; Ehara, M.; Toyota, K.; Fukuda, R.; Hasegawa, J.; Ishida, M.; Nakajima, T.; Honda, Y.; Kitao,O.; Nakai, H.; Klene, M.; Li, X.; Knox, J. E.; Hratchian, H. P.; Cross, J. B.; Bakken, V.; Adamo, C.; Jaramillo, J.; Gomperts, R.; Stratmann, R. E.; Yazyev, O.; Austin, A. J.; Cammi, R.; Pomelli,C.; Ochterski,J. W. ; Ayala, P. Y.; Morokuma, K.; Voth, G. A.; Salvador, P.; Dannenberg, J. J.; Zakrzewski, V. G.; Dapprich, S.; Daniels, A. D.; Strain, M. C.; Farkas, O.; Malick, D. K.; Rabuck, A. D.; Raghavachari, K.; Foresman, J. B.; Ortiz, J. V.; Cui, Q.; Baboul, A. G.; Clifford, S.; Cioslowski, J.; Stefanov, B. B.; Liu, G.; Liashenko, A.; Piskorz, P.; Komaromi, I.; Martin, R. L.; Fox, D. J.; Keith, T.; Al-Laham, M. A.; Peng, C. Y.; Nanayakkara, A.; Challacombe, M.; Gill, P. M. W.; Johnson, B.; Chen, W.; Wong, M. W.; Gonzalez, C.; Pople, J. A. *Gaussian 03*, revision B.04; Gaussian, Inc.: Pittsburgh, PA, 2003.
(41) Khan, N. A.; Khan, A.; Savelkoul, H. F. J.; Benner, R. Inhibition of septic shock in mice by an oligopeptide from the β-chain of human chorionic gonadotrophin hormone. *Hum. Immunol.* **2002**, *63*, 1–7.

(42) Lever, A. B. P. *Inorganic Electronic Spectroscopy*; Elsevier: New York, 1986.
(43) Bencini, A.; Bianchi, A.; Garcia-España, E.; Micheloni, M.; Ramirez, J. A. Proton coordination by polyamine compounds in aqueous solution. *Coord. Chem. Rev.* **1999**, *188*, 97–156.
(44) Johnson, C. K. *ORTEP*; Report ORNL-3794; Oak Ridge National Laboratory: Oak Ridge, TN, 1971.
(45) Matsuba, T.; Creutz, C. Properties and reactivities of pentadentate ethylendiaminetetraacetate complexes of ruthenium(III) and -(II). *Inorg. Chem.* **1979**, *18*, 1956–1966.
(46) Wyllie, G. R. A.; Scheidt, W. R. Solid-state structures of metalloporphyrin NO_x Compounds. *Chem. Rev.* **2002**, *102*, 1067–1090.
(47) Schauer, C. K.; Anderson, O. P. Polydentate chelate. 3. Structures of $EGTA^{4-}$ chelates of manganese(II) and copper(II): $Sr[Mn(EGTA)]\cdot 7H_2O$ and $[Cu_2(EGTA)(OH_2)_2]\cdot 2H_2O$. *Acta Crystallogr.* **1988**, *C44*, 981–986.
(48) Rochelle, L. G.; Morana, S. J.; Kruszyna, H.; Russell, M. A.; Wilcox, D. E.; Smith, R. P. Interactions between hydroxocobalamin and nitric oxide (NO): evidence for a redox reaction between NO and reduced cobalamin and reversible NO binding to oxidized cobalamin. *J. Pharmacol. Exp. Ther.* **1995**, *275*, 48–52.
(49) Kruszyna, H.; Megyar, J. S.; Rochelle, L. G.; Russell, M. A.; Wilcox, D. E.; Smith, R. P. Spectroscopic studies of nitric oxide (NO) interactions with cobalamins: reaction of NO with superoxocobalamin(III) likely accounts for cobalamin reversal of the biological effects of NO. *J. Pharmacol. Exp. Ther.* **1998**, *285*, 665–671.
(50) Wilkins R. G. *Kinetics and Mechanism of Reactions of Transition Metal Complexes*; VCH: Wenheim, Germany, 1991; Chapter 5.
(51) Hay, R. V. Substitution Reactions of Inert-Metal Complexes—Coordination Numbers 6 and Above: Other Inert Centers. In *Mechanisms of Inorganic and Organometallic Reactions*; Twigg, M. V. Ed.; Plenum Press: New York, 1994; Vol. 4, pp 2073−2107.
(52) Burgess, J. *Metal Ions in Solution*; Ellis Horwood Ltd.: Chichester, U.K., 1978.
(53) Morroni, L.; Secco, F.; Venturini, M.; Garcia, B.; Leal, J. M. Kinetics and equilibria of the interactions of hydroxamic acids with gallium(III) and indium(III). *Inorg. Chem.* **2004**, *43*, 3005–12, and references therein.
(54) Moore, P. Inert Metal Complexes: Co-ordination Numbers Six and Higher. In *Inorganic Reaction Mechanisms*; The Chemical Society: London, 1977; Vol. 5, pp 162−239.
(55) Davidson, J. L. Isomerization: Intramolecular Processes. In *Inorganic Reaction Mechanisms*; The Chemical Society: London, 1977; Vol. 5, pp 408−439.
(56) Storr, T.; Cameron, B. R.; Gossage, R. A.; Yee, H.; Skerly, R. T.; Darkes, M. C.; Fricker, S. P.; Bridger, G. J.; Davies, N. A.; Wilson, M. T.; Maresca, K. P.; Zubieta, J. Ru^{III} complexes of edta and dtpa polyaminocarboxylate analogues and their use as nitric oxide scavengers. *Eur. J. Inorg. Chem.* **2005**, 2685–2697.

JM701553U